THE JOURNAL OF PHYSICAL CHEMISTRY B

ARTICLE

pubs.acs.org/JPCB

Spectrally Silent Intermediates during the Photochemical Reactions of *Salinibacter* Sensory Rhodopsin I

Keiichi Inoue,*[,†] Yuki Sudo,[‡,§] Michio Homma,[‡] and Hideki Kandori[†]

[†]Department of Frontier Materials, Nagoya Institute of Technology, Showa-ku, Nagoya 466-8555, Japan

[‡]Division of Biological Science, Graduate School of Science, Nagoya University, Chikusa-ku, Nagoya 464-8602, Japan

[§]PRESTO, Japan Science and Technology Agency (JST), 4-1-8 Honcho Kawaguchi, Saitama, 332-0012, Japan

Supporting Information

ABSTRACT: *Salinibacter* sensory rhodopsin I (*Sr*SRI) is a microbial rhodopsin discovered from the eubacterium *Salinibacter ruber*. It is thought to be a photoreceptor engaging the signal transductions for both positive and negative phototaxis. To elucidate the photoreactions of *Sr*SRI in the presence and absence of chloride ions, we measured the refractive index change after the photoexcitation by the transient grating method. As a result, two spectrally silent processes were identified after the formation of M intermediate, and we named the spectrally identical intermediates M_1, M_2, and M_3. The enthalpy changes (ΔH) were estimated as ΔH = 136, 99, and 63 kJ/mol for K, M_1, and M_2 intermediates, respectively. The ΔH values were significantly decreased (36−55 kJ/mol) by the removal of chloride ions, suggesting their importance for structural changes of *Sr*SRI. Volume expansions of *Sr*SRI were observed on the spectrally silent steps (44 and 11 mL/mol). They may be related to the signaling process because blue-shifted intermediates of sensory rhodopsins are thought to be active state(s) for phototaxis.

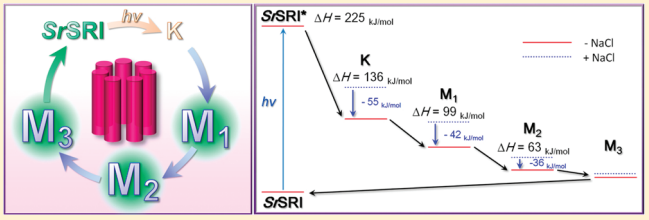

1. INTRODUCTION

A huge number of species of microbes use the light energy from the sun by virtue of pigment proteins located in their plasma membranes. These pigments are called microbial rhodopsins (type 1 rhodopsins), and all of them have heptatransmembrane helical structure and bind the common chromophore *all-trans*-retinal in the transmembrane region.[1] Their biological functions are roughly classified into two groups: light-driven ion transporters and photoreceptors controlling the direction of the flagellar motor rotation or the composition of photosynthetic pigments. In the halophilic archaeon *Halobacterium salinarum*, four microbial rhodopsins were identified. Two of them are light-driven ion pumps bacteriorhodopsin (BR) and halorhodopsin (HR), and the others are photoreceptors for phototaxis signaling (sensory rhodopsins I and II from *Halobacterium salinarum*, *Hs*SRI and *Hs*SRII). *Hs*SRI and *Hs*SRII form stable complexes with each cognate transducer protein (HtrI for SRI and HtrII for SRII) in the plasma membrane. *Hs*SRI is known to be converted to the signaling state evoking attractant behavior of the cells by absorbing orange light. Furthermore, activated *Hs*SRI can absorb second UV light and its photoproduct inversely stimulates the repellent signaling system of the cell.

Most of the structural features and photochemical dynamics of sensory rhodopsins have been obtained in the study of SRII from *Natronomonas pharaonis* (*Np*SRII, also called phoborhodopsin, pR). Because *Np*SRII shows high stability under various conditions including low salt concentration and detergent solubilized state, several structural and spectroscopic studies have been performed to date[2−9] and many aspects of the signaling mechanism of *Np*SRII were revealed. On the other hand, the molecular insights into the structure and dynamics of SRI are much less than those for SRII. One of the largest problems is its lower stability than *Np*SRII. Especially, the low stability at low salt concentration and/or in solubilized condition has made many biochemical and spectroscopic experiments highly difficult. However, this hard situation seems to be overcome by the advent of a new sensory rhodopsin I (named *Sr*SRI) discovered in the eubacterium *Salinibacter ruber*.[10] Abundant expression of *Sr*SRI by *E. coli* is established, the protein shows photochemical properties similar to those of *Hs*SRI and SRI from *Haloarcula vallismortis* (*Hv*SRI),[11] and it shows surprisingly high stability even in the absence of salts. In addition, it can be solubilized by detergent. This indicates that various experiments impossible in the case of *Hs*SRI become possible with *Sr*SRI. Actually, by virtue of its stability, the presence of chloride binding site in the protein moiety was clarified by measuring the salt concentration dependence on both the absorption spectra and decay of the M intermediate.[12]

The photocycle of *Sr*SRI was previously studied by flash photolysis,[10,13] and it was very similar to that of *Hs*SRI.[14] After orange-light absorption by the original state having *all-trans*-retinal as a chromophore, the molecule is converted to a red-shifted K intermediate having 13-*cis*-retinal. The K relaxes to a highly blue-shifted M state in the near-UV region at 24 μs,[13] and finally M

Received: January 4, 2011
Revised: March 10, 2011
Published: March 30, 2011

recovers to the initial state at 170 ms.[10] On the other hand, we can photoconvert M to another intermediate whose absorption maximum locates at 525 nm (P525) by irradiation of UV light. Based on the similarity of this reaction scheme to the photocycle of *Hs*SRI, M and P525 are expected to be the active states transmitting positive and negative phototaxing signals, respectively. However, because the structural insights about the photoactivated intermediates are currently limited, the molecular mechanism of how *Hs*SRI and *Sr*SRI transmit the signals toward their cognate transducers remains unknown. In the literature, it is addressed that the structural changes without any absorption shift of the chromophore are frequently taken into account as an important role in achieving their functions of microbial rhodopsins. For example, a spectrally silent process between M_1 and M_2 intermediates was reported in the BR photocycle and molecular switching indispensible for the proton pumping function of BR occurs in this process.[15,16] There is another spectrally silent process in HR photocycle, L_1 to L_2, and chloride movement from the extracellular to the cytoplasmic side of the protein body was identified in this step.[17] In the case of *Np*SRII, a time-resolved EPR study revealed that the tilting of the F-helix of *Np*SRII considered to be important for the signal transduction to the transducer occurs during the M_1 to M_2 transition.[18] These examples strongly suggest the importance of the studies on spectrally silent processes for the complete understanding of rhodopsin dynamics.

To study the dynamics of spectrally silent processes, several time-resolved measurement methods were applied to rhodopsins. Time-resolved Fourier transform infrared (FTIR) spectroscopy is a very informative method which provides insights into conformational changes at the amino acid level.[16,19−22] Time-resolved UV resonance Raman spectroscopy can detect the conformational changes of amino acid residues far from the chromophore binding pocket.[23−25] On the other hand, time-resolved fluorescence spectroscopy and EPR measurements detect the changes at an arbitrary part of the molecule by using site-directed labeling techniques.[9,18,26] The advent of time-resolved X-ray crystallography made it possible to obtain all-atomic movies of photoreceptor proteins.[27−29] In 2001, a novel technique, the transient grating (TG) method, was reported as a new tool for detecting spectrally silent processes of photoreceptor proteins. The TG method is a third-order nonlinear spectroscopic method measuring the refractive index change (δn) of media after photoirradiation.[30−33] In TG measurement, we cross two pump laser pulses which have identical wavelengths and phases on the sample solution with a 2−60° crossing angle. These pulses make an interference pattern, and the molecules in the sample are space-selectively excited at the position where the two beams positively interfere. If the spectrum and/or the structure of an excited molecule changes after photoactivation, the refractive index of the sample media changes. The periodic spatial distribution of δn can act as an optical grating. Therefore, if we introduce another probe beam satisfying the Bragg condition of the grating, a part of the probe beam is diffracted, and we can measure the degrees of refractive index change of the sample by monitoring the intensity of the diffracted beam. Because δn is closely related to the density change of the media, even if the molecular spectrum does not change, any conformational change which should accompany partial molar volume change (ΔV) can be detected by the TG method via δn. Actually, in the case of photoreactive proteins, the presence of spectrally silent species of many photoreceptor proteins was identified by the TG method.[31,32,34−41]

In this study, we applied the TG method to *Sr*SRI to study the presence of hidden intermediate(s) in its photocycle with and without chloride ions (Cl^-). For that purpose, the TG signal was compared with the result of flash photolysis[10,12] to identify the spectrally silent process of *Sr*SRI. In addition, the TG method can determine the translational diffusion coefficient (D) of the molecule from the q dependence of the decay rate of the signal. Furthermore, ΔH and ΔV of the intermediates were investigated by the TG method in both the presence and absence of chloride ions to study the effect of chloride ion binding on the thermodynamic properties and/or the structural change of *Sr*SRI.

2. MATERIALS AND METHODS

2.1. Protein Expression and Purification. The expression plasmid of *Sr*SRI was constructed as previously described.[10] Cells were grown in LB medium supplemented with ampicillin (final concentration of 50 μg/mL). *E. coli* BL21(DE3) harboring the plasmid was grown to an OD_{660} of 0.3−0.4 in a 30 °C incubator, followed by the addition of 0.5 mM IPTG and 5 μM *all-trans*-retinal. Cells were harvested at 8 h postinduction at 18 °C by centrifugation at 4 °C, resuspended in buffer (50 mM MES, pH 6.5) containing 1 M NaCl, and disrupted by sonication as previously described.[13] Cell debris was removed by a low-speed centrifugation (5000*g* for 10 min at 4 °C). Crude membranes were collected by centrifugation (100000*g* for 30 min at 4 °C) and washed with buffer (50 mM MES, pH 6.5) containing 1 M NaCl. For solubilization of the membranes, 2% (w/v) *n*-dodecyl-β-D-maltoside (DDM) was added and the suspension was incubated for 30 min at 4 °C. The solubilized membranes were isolated by high-speed centrifugation (100000*g* for 30 min at 4 °C), and the supernatant was applied to a Ni-affinity column (HisTrap, GE Healthcare, Uppsala, Sweden) at 4 °C in the dark. Thereafter, the column was washed extensively with buffer (50 mM MES, pH 6.5) containing 1 M NaCl, 20 mM imidazole, and 0.05% w/v DDM to remove unspecifically bound proteins. The histidine-tagged proteins were then eluted using a linear gradient of up to 100% elution buffer (0.05% DDM, 1 M NaCl, 50 mM Tris·Cl, pH 7.0, and 500 mM imidazole). The eluted protein was then further purified by a gel-filtration column, Sephacryl S-400 (GE Healthcare, Uppsala, Sweden), in buffer containing 0.05% DDM, 1 M NaCl, and 50 mM Tris·Cl (pH 7.0). The sample was concentrated and exchanged by Amicon Ultra (Millipore, Bedford, MA, USA) against media with compositions as described below.

2.2. TG Measurement. The principles of the TG method and detailed explanations of experimental setups were previously reported.[30−32,35] We used the nanosecond pulse of second harmonics of a Nd^{3+}:YAG laser (INDI-40-10, Santa Clara, CA, USA; λ = 532 nm, laser power = 100 μJ/pulse) as excitation light. The excitation beam was divided by a beam splitter into two beams. Both beams were aligned to parallel configuration and introduced to a lens (f = 200). The lens focused those beams on the sample cuvette, and they crossed each other on the surface of the cuvette. We used a CW diode (CrystaLaser, Reno, NV, USA; λ = 808 nm) laser as a probe beam, and it was focused by the same lens onto the excited area. The diffraction (TG signal) of the probe beam by a transient grating was isolated by pinholes from the probe beam itself and the scattering of laser beams. The signal was detected by a photomultiplier tube (R10699, Hamamatsu Photonics K. K., Hamamatsu, Japan) equipped with a long pass filter (R66, Sigma-Koki, Tokyo, Japan) and monitored by a digital oscilloscope and recorded in a computer. The laser power

was 500 nJ/pulse, and the repetition rate was 1 Hz, which is sufficiently slower than the turnover rate of the photocycle of *Sr*SRI to avoid multiple excitations. For TG measurement, the purified sample of *Sr*SRI in DDM detergent micelles was resuspended in 50 mM Tris·Cl, pH 7.0, 0.1% DDM, and 1 M NaCl. In the measurement of 0 M NaCl condition, we added 333 mM Na_2SO_4 to adjust the ionic strength of the solvent the same as 1 M NaCl. The protein concentration was ca. 250 μM (optical density = 10 at λ_{max} = 560 nm). The temperature of the sample was kept at 25 °C during the measurement. We did not observe any detectable irreversible bleaching of the sample after each measurement, assuring no damage of protein is caused by photoirradiation. We accumulated >500 signals to obtain low noise signals.

2.3. Determination of Quantum Yield of *Sr*SRI by Flash Photolysis. We used the same buffer as the transient grating measurement for flash photolysis, and the protein concentration was adjusted to 12.5 μM. Flash-induced absorption spectrum changes of *Sr*SRI in the 300−800 nm region were measured and compared with that of BR using a commercial flash photolysis system (Hamamatsu Photonics K. K., Hamamatsu, Japan), which consisted of an ICCD linear detector (Photonic Multichannel Spectral Analyzer PMA-11 C8808-01), a CW xenon lamp L8004 as a light source, and a sample room (flash photolysis optics C9125). The delay time of ICCD was set to 300 μs, at which all excited species converted to M states for both samples, and the gate width was 80 μs. Excitation of the *Sr*SRI samples was done by second harmonics of nanosecond pulsed Nd^{3+}:YAG laser apparatus (INDI-40-10, Santa Clara, CA, USA; λ = 532 nm, laser power = 100 μJ/pulse). The repetition rate of the laser pulses was 1 Hz. Synchronization of data acquisition and laser triggering was performed using delay pulse generators (DG535 and DG645; Stanford Research Systems, Sunnyvale, CA, USA). For signal-to-noise improvement, 100 spectra were averaged for each sample. The quantum yield of *Sr*SRI was determined by comparing the intensities of the bleaching signals of *Sr*SRI and BR, and three sets of identical measurements were performed to estimate the experimental error. The temperature of the sample was kept at 25 °C.

3. PRINCIPLES

3.1. The Principle of TG. Detailed explanations of TG measurement of photoreceptor proteins were reported in previous papers.[30,31,34−36] We will briefly summarize here. If there is no absorption change at the probe wavelength, the intensity of the TG signal is proportional to the square of the refractive index change accompanying the photoreaction.

$$I_{TG} = \alpha\{\delta n(t)\}^2 \quad (1)$$

In the time region longer than nanoseconds, $\delta n(t)$ is composed of the refractive index changes resulting from different origins. The first one is the density change of the media by thermal expansions caused by the heat released from excited molecules (thermal grating, $\delta n_{th}(t)$). The second is the population grating ($\delta n_{pop}(t)$) accompanying the absorption change of the sample in accordance with the Kramers−Krönig relationship. Refractive index change caused by partial molar volume change (ΔV) of excited molecules also contributes to δn (volume grating, $\delta n_{vol}(t)$). The sum of $\delta n_{pop}(t)$ and $\delta n_{vol}(t)$ is called the species grating ($\delta n_{spe}(t)$), because both $\delta n_{pop}(t)$ and $\delta n_{vol}(t)$ are related to the properties of molecular species. Therefore, we can express $\delta n(t)$ as follows:

$$\begin{aligned}\delta n(t) &= \delta n_{th}(t) + \delta n_{spe}(t) \\ &= \delta n_{th}(t) + \delta n_{pop}(t) + \delta n_{vol}(t)\end{aligned} \quad (2)$$

The decay of a TG signal is governed by the diffusion processes and the recovery reaction to the initial state. If we consider the simplest photocycle, in which the reactant (R) is photoconverted to the product (P) and P thermally recovers to R, the species grating becomes

$$\delta n_{spe}(t) = (\delta n_{spe,P} - \delta n_{spe,R}) \exp(-(Dq^2 + 1/\tau_{rec})t)^2 \quad (3)$$

where $\delta n_{spe,P}$ and $\delta n_{spe,R}$ are the species gratings of P and R; D, q, and τ_{rec} are the translational diffusion coefficient of the molecule, the grating wavenumber of the transient grating, and the time constant of the recovery process, respectively. q is determined by the crossing angle of the pump beams and their wavelength ($q = 4\pi \sin(\theta/2)/\lambda_{ex}$). Equation 3 implies that we can determine D and $1/\tau_{rec}$ by plotting the decay rate of the TG signal against the q^2 value whose slope and intercept at $q^2 = 0$ correspond to them, respectively.

On the other hand, the temporal evolution of δn_{th} represents the generation and diffusion of the released heat from the excited molecule, and one can express it as

$$\delta n_{th}(t) = \left(\frac{dn}{dT}\right)\frac{W}{\rho C_P}\left[\frac{dQ(t)}{dt} \otimes \exp(-D_{th}q^2 t)\right] \quad (4)$$

where T, W, ρ, C_P, and D_{th} are temperature, the molecular weight, the density, the heat capacity at constant pressure, and the thermal diffusion coefficient of the solvent, respectively. The symbol "⊗" represents the convolution integral, and $Q(t)$ is heat-releasing process from the excited molecule. In the case of the simple photoreaction of R → P, if the heat release finishes much faster than the instrumental time resolution, $Q(t)$ is expressed by a Dirac delta function, $\delta n_{th}\ \delta(t)$, and the $\delta n_{th}(t)$ becomes a uniformly decaying exponential function whose amplitude and decay rate are δn_{th} and $D_{th}q^2$, respectively. If the enthalpy difference of P from the initial state is ΔH and the reaction quantum yield is Φ, the thermal grating signal accompanying P formation ($\delta n_{th,P}$) is expressed as

$$\delta n_{th,P} = \left(\frac{dn}{dT}\right)\frac{h\nu W}{\rho C_P}\left(1 - \frac{\Phi\Delta H}{h\nu}\right)\Delta N \quad (5)$$

where $h\nu$ and ΔN are the energy of the pump photon and the number of excited molecules in unit volume, respectively. If we measure the thermal grating signal of the calorimetric reference reagent which releases all absorbed photon energy to solvent much faster than the instrumental time resolution and the absorbance of the reference is precisely the same as that of the sample protein, the intensity of the thermal grating of the reference ($\delta n_{th,ref}$) becomes

$$\delta n_{th,ref} = \left(\frac{dn}{dT}\right)\frac{h\nu W}{\rho C_P}\Delta N \quad (6)$$

and the ratio between $\delta n_{th,P}$ and $\delta n_{th,ref}$ is expressed as

$$\frac{\delta n_{th,P}}{\delta n_{th,ref}} = 1 - \frac{\Phi\Delta H}{h\nu} \quad (7)$$

Equation 7 means that one can determine the $\Phi\Delta H$ of the product molecule by comparative TG measurement with the calorimetric reference. Therefore, if Φ is determined by another measurement, ΔH of the product species is obtained. In the case of photoreceptor

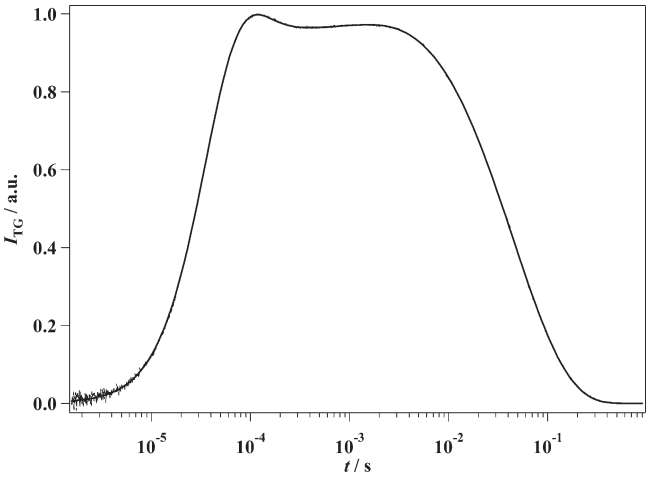

Figure 1. TG signal of *Sr*SRI in 1 M NaCl at $q^2 = 1.06 \times 10^{11}$ m^{-2} (dashed line) and fitting line based on eq 9 (solid line).

proteins, the temporal profile of $Q(t)$ is more complicated and we show the complete expression of $\delta n_{th}(t)$ for the photoreaction process of *Sr*SRI in section 4.2.

The intensity of the volume grating, δn_{vol}, can also be quantitatively expressed. If the partial molar volume of the molecule increases in the R → P process, the volume grating on the production of P, $\delta n_{vol,P}$, is given by

$$\delta n_{vol,P} = -\frac{(n_0^2+2)^2}{18 n_0 \varepsilon_0}\frac{\alpha_{solv}}{V_{solv}}\Phi \Delta V \Delta N \qquad (8)$$

where n_0, ε_0, α_{solv}, and V_{solv} are the refractive index of solvent, the permittivity of free space, the coefficient of thermal expansion, and the partial molar volume of the solvent, respectively. Therefore, we can obtain the absolute value of ΔV by calculating the ratio between δn_{vol} and $\delta n_{th,ref}$, and employing the literature value of the physical constants of the solvent on the right sides of eqs 6 and 8 and the value of the reaction quantum yield.

4. RESULTS

4.1. TG Measurement of *Sr*SRI. The TG signal of *Sr*SRI is shown in Figure 1 with 532 nm excitation and 808 nm probe wavelengths at $q^2 = 1.06 \times 10^{11}$ m^{-2}. After the first rise in the microseconds to several tens of microseconds time region, a small decay around $t = 200$ μs and second small rising signal around 1 ms were observed. Then, the signal decayed to zero in the several tens of milliseconds to 100 ms time region. We fitted the signal by a sum of exponential functions, and six exponentials were required to reproduce the signal (solid line in Figure 1). Further addition of exponential terms did not improve the residuals of the fitting, and the time constant of newly added components converged to that of another component. This indicates that the number of significant components of the TG signal is 6 and it is expressed as

$$I_{TG} = \left\{\sum_{i=1}^{6} \delta n_i \exp(-t/\tau_i)\right\}^2 \qquad (9)$$

where δn_i and τ_i $(i = 1-6)$ are the preexponential factor and time constant of each component, respectively.

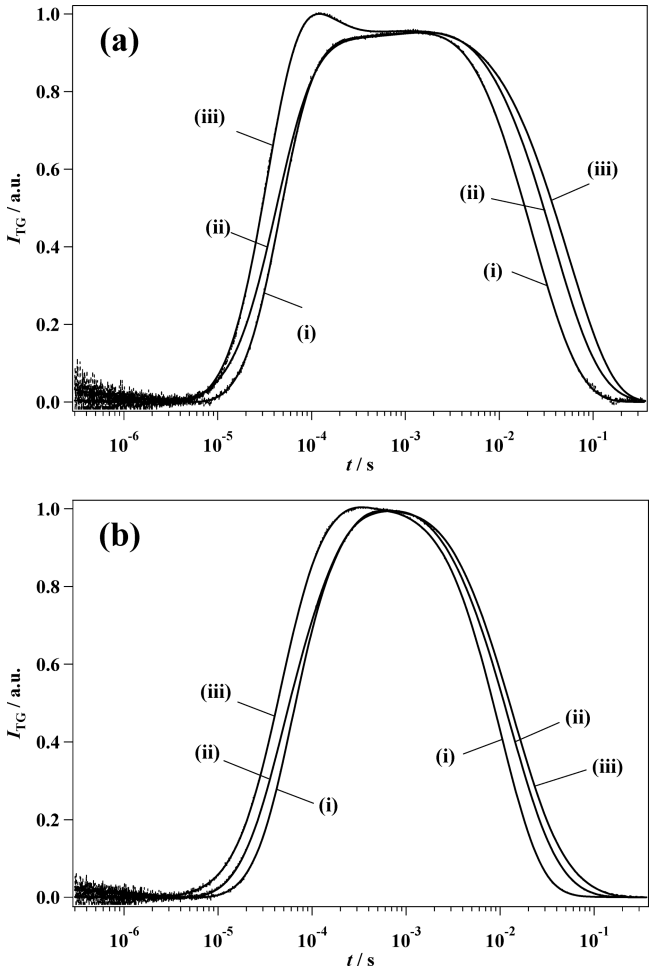

Figure 2. (a) TG signals of *Sr*SRI in 1 M NaCl at (i) $q^2 = 8.74 \times 10^{11}$ m^{-2}, (ii) $q^2 = 2.87 \times 10^{11}$ m^{-2}, and (iii) $q^2 = 8.77 \times 10^{10}$ m^{-2} (dashed lines) and fitting lines based on eq 9 (solid lines). (b) TG signals of *Sr*SRI in 0 M NaCl at (i) $q^2 = 7.39 \times 10^{11}$ m^{-2}, (ii) $q^2 = 1.69 \times 10^{11}$ m^{-2}, and (iii) $q^2 = 5.07 \times 10^{10}$ m^{-2} (dashed lines) and fitting lines to them based on eq 9 (solid lines).

Next, we changed the crossing angle of the two pulse beams. This changes the grating wavenumber of the transient grating, and it is related to the crossing angle as $q = 4\pi \sin(\theta/2)/\lambda_{ex}$, where θ and λ_{ex} are the crossing angle of the pump beams and the pump wavelength, respectively. The signals at three different q^2 values ($q^2 = 8.74 \times 10^{11}$, 2.87×10^{11}, 8.77×10^{10} m^{-2}) are shown in Figure 2a. All of these signals were also reproduced by a sum of six exponentials. However, the time constants of two of them were dependent on the q^2 value and they became faster at higher q. The time constant of one of the q^2-dependent components was identical to that of the thermal grating signal of the calorimetric reference (Evans Blue) ($\tau_{th} = 1/D_{th}q^2$). Therefore, we assigned this component to the thermal grating of the released heat from an excited *Sr*SRI molecule. Because the refractive index change of the thermal grating ($\delta n_{th,SrSRI}$) must be negative at this temperature, we could determine the signs of δn_i's of the other five components as $\delta n_1 > 0$, $\delta n_2 > 0$, $\delta n_3 > 0$, $\delta n_4 < 0$, and $\delta n_5 < 0$, respectively, based on their relative sign to $\delta n_{th,SrSRI}$. These components represent the refractive index change originated from the presence and dissipation of chemical species and they are called the population grating, δn_{spe} (see section 3).

dx.doi.org/10.1021/jp2000706 |*J. Phys. Chem. B* 2011, 115, 4500–4508

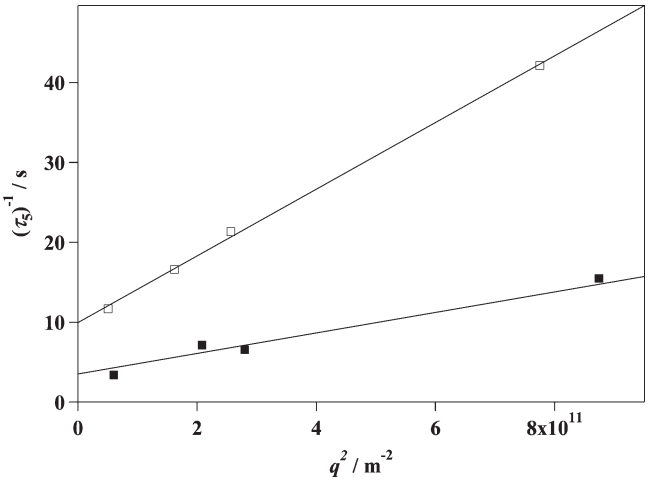

Figure 3. Inversion of τ_5 vs q^2 plot with 1 M NaCl (filled squares) and without NaCl (open squares). Solid lines represent the best fitted lines based on eq 3. The slopes and intercepts at $q^2 = 0$ of each line correspond to molecular diffusion coefficients and rate constants, respectively.

Table 1. Time Constants of the Exponents Included in TG Signals in 1 and 0 M NaCl

salt concn	τ_1 (μs)	τ_2 (μs)	τ_3 (ms)	τ_4 (ms)	τ_{rec} (ms)	D (10^{-11} m^2 s^{-1})
1 M NaCl	24 ± 3	60 ± 12	1.8 ± 0.3	57 ± 17	280 ± 40	1.28 ± 0.05
0 M NaCl	28 ± 3	91 ± 18	1.3 ± 1.1	22 ± 2	101 ± 4	4.17 ± 0.10

The TG signal of *Sr*SRI in the solution without NaCl is shown in Figure 2b ($q^2 = 7.39 \times 10^{11}$, 1.69×10^{11}, 5.07×10^{11} m^{-2}). (Throughout this paper, 333 mM Na_2SO_4 was added to the solvent for the 0 M NaCl experiment to adjust the ionic strength the same as 1 M NaCl.) While the signal in the fast time region was very similar to that of 1 M NaCl, the decay rate of the signals became much faster. These signals also were well fitted by a sum of of six exponentials, and one of them was assigned to the thermal diffusion grating as the 1 M NaCl condition. While the signs of preexponential factors were the same as in the 1 M NaCl condition, some of these time constants were significantly different from the 1 M NaCl results. The time constant of the slowest species grating component (τ_5) of both salt conditions also depended on the q^2 value (second q^2-dependent component). This indicates that there are contributions of molecular diffusion to the elimination of the transient grating. Additionally, the recovery process of *Sr*SRI to the initial state was reported to occur in this time region.[10] In this case, τ_5 can be expressed as $1/\tau_5 = 1/\tau_{rec} + Dq^2$, where τ_{rec} and D are the intrinsic recovery rate of the photocycle and the translational molecular diffusion coefficient, respectively.[35] The plots of inversion of τ_5 against q^2 are shown in Figure 3. For both salt conditions, we observed good linear correlations and diffusion coefficients of τ_{rec} and *Sr*SRI (D) were determined to be 280 ± 40 ms and $(1.28 \pm 0.05) \times 10^{-11}$ m^2/s in 1 M NaCl and 101 ± 4 ms and $(4.17 \pm 0.10) \times 10^{-11}$ m^2/s in the solution without NaCl, respectively. The lifetimes of all reaction components determined by TG signals and diffusion coefficients with and without NaCl are summarized in Table 1.

We previously reported the photochemical reaction dynamics of *Sr*SRI by using conventional flash photolysis apparatus.[12] The lifetime of K was reported as 24 ± 4 μs, and the decay of M showed double exponential behavior whose lifetimes were 66.7 ± 1.5 and 240 ± 30 ms in 1 M NaCl. (Although we analyzed the M decay with a single exponential function in a previous report, further analysis found that it is more precisely reproduced by a double exponential function (see the Supporting Information).) While the K decay did not show a significant difference, only the M decay was fastened in the absence of Cl^- ions (22 ± 8 μs for K decay and 27.1 ± 1.4 and 100 ± 20 ms for M decay in 0 M NaCl). The values of these lifetimes were identical to the τ_1, τ_4, and τ_{rec} determined by the TG method both in 1 and 0 M NaCl. Therefore, we assigned the components of τ_1, τ_4, and τ_{rec} to K → M and double exponential M → *Sr*SRI recovery processes. On the other hand, the τ_2 and τ_3 components were exclusively observed in the TG signal and no absorption change was observed from M in flash photolysis measurement.[12] This indicates all of the second to fourth intermediates identified by the TG method have identical blue-shifted absorption spectra. As result, we concluded that τ_2 and τ_3 are spectrally silent reaction processes among three substates of M and we name them M_1, M_2, and M_3. In the case of spectrally silent processes, the TG signals corresponding to them exclusively originate from volume change of the protein molecule volume grating.[35−37] Therefore, the M_1, M_2, and M_3 observed in the TG signal have different partial molar volumes and their structures are different from each other. The absolute values of volume difference among the M substate can be quantitatively determined by the comparison with the thermal grating signal of the calorimetric reference (see below).

4.2. Quantitative TG Measurement. In the q range of our current experimental conditions ($q^2 = 1 \times 10^{12} - 8 \times 10^{10}$ m^{-2}), the preexponential amplitude of the thermal grating signal of *Sr*SRI, $\delta n_{th,SrSRI}$, is expressed as

$$\delta n_{th,SrSRI} = \delta n_{th,K} + \frac{k_K}{k_K - D_{th}q^2}\delta n_{th,L} + \frac{k_K k_L}{k_L - k_K}\left(\frac{1}{k_K - D_{th}q^2} - \frac{1}{k_L - D_{th}q^2}\right)\delta n_{th,M} \quad (10)$$

where $\delta n_{th,K}$, $\delta n_{th,M_1}$, and $\delta n_{th,M_2}$ are the thermal grating signals generated on the K formation, K → M_1, and M_1 → M_2 processes, respectively.[31,34,35] Equation 10 indicates that the amplitude of the thermal grating signal obtained from the fitting in Figure 2 depends on q^2 and we can decompose the $\delta n_{th,K}$, $\delta n_{th,M_1}$, and $\delta n_{th,M_2}$. These components are expressed as

$$\delta n_{th,K} = \left(\frac{dn}{dT}\right)\frac{h\nu W}{\rho C_P}\left(1 - \frac{\Phi_{SrSRI}\Delta H_K}{h\nu}\right)\Delta N \quad (11)$$

$$\delta n_{th,M_1} = \left(\frac{dn}{dT}\right)\frac{W}{\rho C_P}\Phi_{SrSRI}(\Delta H_K - \Delta H_{M_1})\Delta N \quad (12)$$

$$\delta n_{th,M_2} = \left(\frac{dn}{dT}\right)\frac{W}{\rho C_P}\Phi_{SrSRI}(\Delta H_{M_1} - \Delta H_{M_2})\Delta N \quad (13)$$

where $h\nu$, W, ρ, C_P, Φ_{SrSRI}, and ΔN are the energy of the pumping photon, the molecular weight, the density, the heat capacity at constant pressure of solvent, the reaction quantum yield, and the number of excited molecules in a unit volume. ΔH_K, ΔH_{M_1}, and ΔH_{M_2} are relative enthalpies of K, M_1, and M_2 from dark state, respectively. The intensity of the thermal grating signal of the calorimetric reference obtained with identical

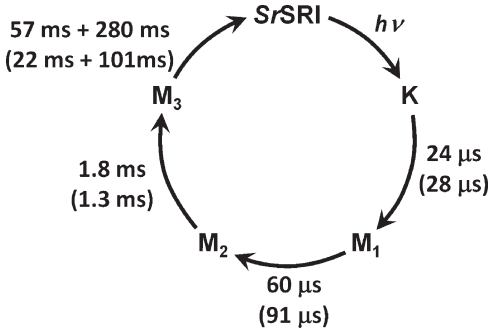

Figure 4. Schematic diagram of the photocycle of *Sr*SRI with 1 M NaCl and without NaCl (in parentheses) including spectrally silent intermediates identified by the TG method.

conditions to *Sr*SRI is expressed by eq 6. Therefore, taking the ratios of $\delta n_{th,K}/\delta n_{th,ref}$, $\delta n_{th,M_1}/\delta n_{th,ref}$, and $\delta n_{th,M_2}/\delta n_{th,ref}$, we can calculate the values of $\Phi_{SrSRI}\Delta H_K$, $\Phi_{SrSRI}\Delta H_{M_1}$, and $\Phi_{SrSRI}\Delta H_{M_2}$.

To obtain the absolute values of these ΔH's, we need another experiment to determine Φ_{SrSRI}. For this purpose, we performed comparative flash photolysis with bacteriorhodopsin (BR) as reported by Losi et al.[42] After the decay of K intermediate, all excited *Sr*SRI converts to M. In this case, the bleaching signal at longer wavelength purely represents the depletion of dark state. The absorption change of the bleaching at a certain wavelength, λ, which is sufficiently longer than absorption of M is given by $\Delta A_{SrSRI,\lambda} = -\varepsilon_{SrSRI,\lambda}\Phi_{SrSRI}(\Delta C)l$, where $\varepsilon_{SrSRI,\lambda}$ is the extinction coefficient of dark state *Sr*SRI at λ and ΔC and l are concentration of reacted molecule and the optical path length of probe light, respectively. On the other hand, BR also accumulates only M intermediate in a submillisecond time window. Therefore, if we measure the transient absorption spectrum of BR whose optical density is adjusted to the same as *Sr*SRI at pumping wavelength, its absorption change of the bleaching of the initial state at λ' which is sufficiently longer than wavelength of M absorption is given by $\Delta A_{BR,\lambda'} = -\varepsilon_{BR,\lambda'}\Phi_{BR}(\Delta C)l$. If we calculate the ratio between $\Delta A_{SrSRI,\lambda}$ and $\Delta A_{BR,\lambda'}$, it becomes

$$\frac{\Delta A_{SrSRI,\lambda}}{\Delta A_{BR,\lambda'}} = \frac{\varepsilon_{SrSRI,\lambda}\Phi_{SrSRI}}{\varepsilon_{BR,\lambda'}\Phi_{BR}} \quad (14)$$

The result of the comparative flash photolysis experiment is shown in Figure 5. The extinction coefficient of BR at λ_{max} = 560 nm, $\varepsilon_{BR,560}$, is 63 000 M^{-1} cm^{-1} and Φ_{BR} = 0.64, respectively.[43,44] The $\varepsilon_{SrSRI,\lambda}$ at λ_{max} = 556 nm was determined as $\varepsilon_{SrSRI,556}$ = 39 005 M^{-1} cm^{-1} by hydroxylamine bleaching of *Sr*SRI and comparison of the absorptions of initial *Sr*SRI and generated retinal oxime (ε = 33 600 M^{-1} cm^{-1} at 360 nm) in 1 M NaCl (data not shown). Based on the results shown in Figure 5, the ratio of the absorption change of *Sr*SRI at 556 nm ($\Delta A_{SrSRI,556}$) and BR at 560 nm ($\Delta A_{BR,560}$) became $\Delta A_{SrSRI,556}/\Delta A_{BR,560}$ = 0.42 ± 0.02. Therefore, by making use of eq 14 and the values of $\varepsilon_{SrSRI,556}$, $\varepsilon_{BR,560}$, and Φ_{BR}, we calculated the reaction quantum yield of *Sr*SRI as Φ_{SrSRI} = 0.44 ± 0.03. With the values of $\Phi_{SrSRI}\Delta H$ for each intermediate obtained from the ratios between thermal grating signals of *Sr*SRI and the calorimetric reference (vide supra) and Φ_{SrSRI}, we determined the enthalpy differences of K, M_1, and M_2 from the initial state of *Sr*SRI, and they are summarized in Table 2. Unfortunately, ΔH of M_3 (ΔH_{M_3}) could not be determined. This is because, although we must make the decay of the thermal grating signal slower than the formation of M_3

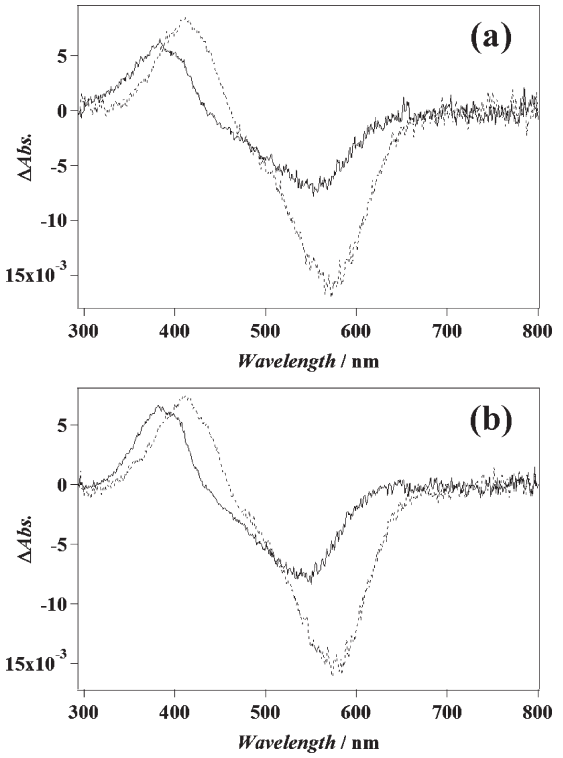

Figure 5. Transient absorption spectra of *Sr*SRI (solid lines) and BR (dashed lines) obtained with identical excitation laser power (100 μJ/pulse) and identical initial dark state absorption at excitation wavelength with 1 M NaCl (a) and without NaCl (b).

Table 2. Enthalpy Changes of K, M_1, and M_2 Intermediates in 1 and 0 M NaCl

salt concentration	ΔH_K (kJ/mol)	ΔH_{M_1} (kJ/mol)	ΔH_{M_2} (kJ/mol)
1 M NaCl	136 ± 17	99 ± 18	63 ± 18
0 M NaCl	81 ± 12	57 ± 13	27 ± 14

to determine ΔH_{M_3}, the formation rate of M_3 (1.8 ms) is much slower than the longest decay of the thermal grating signal which can be achieved by our current instrumental setup (~500 μs). ΔH of K intermediate was 136 ± 17 kJ/mol, and this is surprisingly similar to that of K intermediate of *Hs*SRI (ΔH = 142 ± 12 kJ/mol) reported by Losi et al.[42] This indicates that the energetic features of K intermediates for SRIs derived from different species are similar to each other. This similarity assures that the precision of ΔH values obtained by the TG method is convincing to compare with the results of other techniques.

To study the effect of Cl^- binding on the energy surface of the photoreaction of *Sr*SRI, we conducted similar quantitative TG experiments in the solution without NaCl. At this salt concentration, the wavelength of the absorption maximum, λ_{max}, and the extinction coefficient of *Sr*SRI at λ_{max} slightly change to 542 nm and 40 040 M^{-1} cm^{-1}, respectively. With the values of these quantities and identical flash photolysis experiments to those of 1 M NaCl, we determined Φ_{SrSRI} to be 0.55 ± 0.04 without NaCl. As a result, ΔH values of K, M_1, and M_2 intermediates in the solution without NaCl could be determined, which are shown and compared with those in 1 M NaCl in Table 2 and Figure 6. ΔH's of all studied intermediates were by 55, 42, and 36 kJ/mol

dx.doi.org/10.1021/jp2000706 |J. Phys. Chem. B 2011, 115, 4500–4508

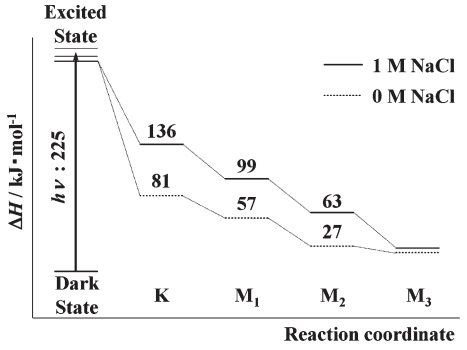

Figure 6. Enthalpy changes (ΔH) of early intermediates of *Sr*SRI. Solid and dashed lines are with 1 M NaCl and without NaCl, respectively. ΔH of M_3 cannot be determined by the TG method (see text).

decreased on K, M_1, and M_2 by the removal of Cl^-, respectively, and Cl^- has the role of increasing the enthalpies of those intermediates.

$M_1 \rightarrow M_2$ and $M_2 \rightarrow M_3$ processes do not accompany any spectrum shift. Therefore, while the contribution of the population grating is negligible in the refractive index change along these processes (δn_2 and δn_3), they can exclusively be assigned to the volume grating.[35−37] The intensity of the volume grating signal is given by eq 8. Therefore, we can calculate the partial molar volume change of protein (ΔV) by taking the ratio between δn_{vol} (eq 8) and $\delta n_{th,ref}$ (eq 6) and using the literature value of other physical constants and quantum yields of each sample determined above. As the result, the partial molar volume changes of *Sr*SRI on M_1 to M_2 and M_2 to M_3 ($\Delta V_{M_1\text{-to-}M_2}$ and $\Delta V_{M_2\text{-to-}M_3}$) were determined to be 44 ± 22 and 11 ± 5 mL/mol in 1 M NaCl, respectively. These results indicate that the partial molar volumes of *Sr*SRI expand on both of two spectrally silent processes. Furthermore, we measured $\Delta V_{M_1\text{-to-}M_2}$ and $\Delta V_{M_2\text{-to-}M_3}$ without NaCl and they were 65 ± 15 and 9 ± 2 mL/mol. Although $\Delta V_{M_1\text{-to-}M_2}$ seems to be larger in the absence of Cl^- ion, there was no significant difference of ΔV values between with Cl^- and without Cl^- within experimental error.

5. DISCUSSION

We studied the dynamics of the photoreaction cycle of *Sr*SRI by the TG method in this paper. Temporal observation of the refractive index change along the reaction identified two new reaction steps additional to the temporal absorption change studied by flash photolysis.[11−13] These spectrally silent processes appeared in the time region where only absorption of M was observed. Therefore, we assigned these processes to the conversion among M-like intermediates and named them M_1 to M_2 and M_2 to M_3. The number of substates of M is the same as that of *Np*SRII reported previously.[35] This implies that the reaction processes of M of these photosensors possess some common features. However, the rates of both $M_1 \rightarrow M_2$ and $M_2 \rightarrow M_3$ of *Np*SRII are about 10 times slower than those of *Sr*SRI, suggesting kinetic differences between positive and negative phototaxis sensors.

We succeeded in determining the relative enthalpies of K, M_1, and M_2 intermediates in both the presence and absence of Cl^-. The ΔH of K intermediate in the presence of Cl^- was similar to that of *Hs*SRI reported previously[42] and it gradually decreased along the reaction coordinate, that is $\Delta H_K > \Delta H_{M_1} > \Delta H_{M_2}$. All of these values became smaller by 36−55 kJ/mol under the no Cl^- condition. Therefore, the energy surface of *Sr*SRI is significantly affected by the binding of the Cl^-. Furthermore, the reduction of ΔH for all intermediate suggests that the Cl^- remains to be bound during the photocycle. This is also supported by the absence of the component of released Cl^- diffusion in contrast to *N. pharaonis* halorhodopsin which releases and rebinds a Cl^- ion during its photocycle.[45] Because the high-resolution structure of SRI was not reported, we could not discuss the detailed position and structure of the Cl^- binding site. However, Suzuki et al. reported that Cl^- binds to His131 located near the β-ionone ring of chromophore retinal.[12] Furthermore, they mentioned that the cavity of a Cl^- binding site should be narrow on the basis of the model structure of *Hs*SRI.[46] This indicates that the configuration of surrounding amino acids and the structure of β-ionone ring and polyene chain of the retinal are distorted by Cl^- binding, and a tightly packed environment would restrict the movement accompanying the reorientation and structural relaxation of 13-*cis*-retinal and amino acid residues around the Cl^- binding pocket. This perturbation changes the energy surface of the molecule and should affect the reaction pathway and/or the turnover rate of *Sr*SRI which is important for signal transduction.

The diffusion coefficient of *Sr*SRI was $(1.28 \pm 0.05) \times 10^{-11}$ m^2/s in 1 M NaCl. If we consider the molecular weight of *Sr*SRI (MW = 26.7 kDa), this value is surprisingly small. Previously, Young and Carroad studied the relationship between the diffusion coefficients and molecular weights (M) of globular protein molecules with more than 300 different proteins.[47] They found that the relationship is expressed as $D = 8.34 \times 10^{-8}(T/\eta M^{1/3})$, where η is the viscosity of solvent. On the basis of this equation and D of *Sr*SRI, we calculated the apparent molecular weight of *Sr*SRI to be 10 400 ± 400 kDa. This is more than 300 times larger compared to the actual molecular weight of *Sr*SRI. What is the origin of this discrepancy? One would consider that it is the effect of the detergent molecules solubilizing the protein. In this case we used DDM as a detergent, whose molecular weight is 510 Da. In general, the number of detergent molecules surrounding the membrane proteins whose size is similar to *Sr*SRI is expected to be ca. 150−200.[48] If this is the case, the total molecular weight of *Sr*SRI and surrounding DDM becomes 106−131 kDa and the apparent molecular weight implies 81−101 *Sr*SRI forms higher aggregates even in detergent solubilized condition. On the other hand, when we decreased the salt concentration to 0 mM NaCl, the diffusion coefficient strongly increased to $(4.17 \pm 0.10) \times 10^{-11}$ m^2/s. In this case, the estimated number of *Sr*SRI molecules in a particle is two to three. This result of the effect of the salt concentration indicates that higher aggregates are formed by hydrophobic interaction between *Sr*SRI molecules which is strengthened by the salting-out effect of NaCl. The similar effect of the solvent condition on D was reported for *Np*SRII. While the D of *Np*SRII was $(3.4 \pm 1.3) \times 10^{-11}$ m^2/s at 4 M NaCl,[35] it increased to $(7.7 \pm 1.2) \times 10^{-11}$ m^2/s at 300 mM NaCl (the latter value is obtained for D75N mutant of *Np*SRII).[36] Therefore, the increase in D at higher salt concentration seems to be a general feature of microbial rhodopsins. Of note, *Sr*SRI forms estimated dimer and trimer even in the SDS-solubilized state.[13]

Although there is the possibility that the relationship of Young and Carroad is not able to be directly applied to membrane proteins and the actual number of molecules is different from the above estimation, according to our measurements, *Sr*SRI is surely in a huge aggregate with an apparently large total molecular weight. Furthermore, the shape of the aggregation also would affect the D. In the case of BR, it is known to form a trimer in purple membrane by contacting transmembrane surfaces of

respective molecules. This indicates the possibility that rhodopsins would lie side-by-side each other even in the detergent. In such a case, the shape of the higher oligomer should be flattened. Perrin theoretically derived the friction ratio between the oblate particle (f) and the spherical one (f_0) as

$$\frac{f}{f_0} = \frac{(a^2/b^2 - 1)^{1/2}}{(a/b)^{2/3} \tan^{-1}(a^2/b^2 - 1)^{1/2}} \quad (15)$$

where a/b is the ratio between the radii along the semimajor (a) and minor (b) axes of the particle.[49,50] If we assume the highly flattened aggregate with $a/b = 5$, f/f_0 is calculated to be 1.22. This indicates that the observed D becomes 1.22 times smaller than the spherical particle which has the same volume. In this case, although the estimated aggregation number decreases to 55−44 molecules, it is still large. We think the actual value of a/b of *Sr*SRI aggregate is smaller and the effect of the shape of aggregate is not so significant. Therefore, we would conclude that the unexpected smaller D of *Sr*SRI is caused by the large number of molecules in the aggregate.

In many studies on photoreceptor proteins by the TG method, diffusion coefficient change is reported to sensitively reflect the conformational change of the molecule.[36−41] To reveal there are diffusion coefficient sensitive conformational changes in the photocycle of *Sr*SRI, we need to perform the measurements with a completely dissociate condition (at least smaller than dimer or trimer). For this purpose, optimization of the salt concentration and/or changing detergent type will be required. Interestingly, when the *Sr*SRI forms a tight complex with *Sr*HtrI, dimer is significantly stabilized in the SDS-solubilized state in addition to the monomer.[13] It has been reported that the dimer of *H. salinarum* HtrI is sandwiched between two molecules of *Hs*SRI[51] and that MCPs including HtrI and HtrII form homodimers in the membrane.[52,53] We speculated that the SDS-resistant homodimer of *Sr*SRI−*Sr*HtrI may be a functionally important form. Thus the complex may overcome the problem. However, it was hard to do similar experiments because of the instability. Further progress is required.

In previous reports Losi et al. reported the ΔH of K intermediate of *Np*SRII[42] and Inoue et al. studied the enthalpy change of early intermediates of *Np*SRII in the presence and absence of transducer protein (*Np*HtrII).[35] The ΔH_K of *Np*SRII is 134 ± 11 kJ/mol,[54] which is also identical to ΔH_K values of *Sr*SRI (136 kJ/mol) and *Hs*SRI (142 ± 12 kJ/mol) within experimental error. Additionally, the first intermediate of octopus rhodopsin, Batho, has a similar enthalpy, ΔH = 146 ± 15 kJ/mol.[55] These results show the universal aspect of K intermediate, which possesses a relatively higher enthalpy (~65% of photon energy of λ_{max} in the case of *Sr*SRI), and it would be a driving force of subsequent photoreactions. In early intermediates, the energy mainly remains around the chromophore binding pocket and the similar ΔH values indicate that the degrees of steric repulsion between the isomerized chromophore and surrounding amino acids were not very different among several proteins.

Partial molar volume changes were observed in $M_1 \rightarrow M_2$ and $M_2 \rightarrow M_3$ processes, and this shows that there are conformational changes of the protein among three M intermediates. The partial molar volume expansion mainly represents the increase of the solvent exclusion volume. We can consider the two types of conformational changes of protein molecule as the origin of partial molar volume expansion as follows: (1) rearrangement around the retinal chromophore leading to the change of the steric and electrostatic force field of the retinal binding pocket; (2) the increase of the solvent-excluded volume by the exposure of closely packed surfaces of molecules. We mentioned the higher aggregation of *Sr*SRI above, and one can expect that the shape and/or the number of the aggregation change would affect the partial molecular volume. However, if the aggregation state is changed, D is also affected. Because the signal of D change is generally very large, TG is very sensitive to it and even a slight difference less than 10% was reported, previously.[39,41] In this study, we observed no signal of D change, and the aggregation state of *Sr*SRI was not transiently changed. Therefore, we can exclude the possibility of the contribution of the change of aggregation state on the partial volume changes among the substates of M.

In previous paper, similar expansions of partial molar volume were reported for *Np*SRII (8.8 mL/mol on $M_1 \rightarrow M_2$, 8.5 mL/mol on $M_2 \rightarrow M_3$), which produces a negative phototaxis signal after photoexcitation.[35] Octopus rhodopsin also shows a spectrally silent process on a later intermediate, Transient Acid Meta → Acid Meta.[55] This process also shows 32 ± 3 mL/mol expansion and the volume changes on other processes were rather small. They suggested the possibility that this volume expansion represents the helix arrangement. Interestingly, all photosensors showed volume expansion on their putative signaling states. To clarify the relationship between the formation of signaling conformation and the volume expansion, we need a further encompassing study in combination with other spectroscopic and biochemical techniques.

6. CONCLUSIONS

In this paper we studied the photocycle of *Salinibacter* sensory rhodopsin (*Sr*SRI) I by the transient grating (TG) method. The results showed the presence of spectrally silent reaction steps after M formation, and three different substates of M were identified. The enthalpy differences (ΔH's) of K, M_1, and M_2 intermediates from unphotolyzed state were determined, and they monotonically decreased along the photocycle. All these enthalpies were significantly decreased by the binding of chloride ion(s). This indicates that the chloride ion affects the energy surface of the *Sr*SRI reaction pathway and Cl^- does not dissociate from the protein molecule in the photocycle. On the other hand, the partial molecular volume of *Sr*SRI increased in the steps of $M_1 \rightarrow M_2$ and $M_2 \rightarrow M_3$ and it was not affected by the binding of Cl^-. We think the ΔV of spectrally silent processes would represent the conformational change important for the signal transduction toward the transducer protein. Because the binding of chloride near the chromophore did not affect the value of ΔV, this molecular expansion should occur on the site far from the retinal binding site. It is likely that M_3 is the signaling state of *Sr*SRI.

■ ASSOCIATED CONTENT

Supporting Information. Analysis of the transient absorption change accompanying the M decay obtained by flash photolysis is described. We compare the results of single and double exponential analyses. This material is available free of charge via the Internet at http://pubs.acs.org.

■ AUTHOR INFORMATION

Corresponding Author

*Tel.: +81-52-753-5224. Fax: +81-52-753-5224. E-mail: inoue.keiichi@nitech.ac.jp.

■ ACKNOWLEDGMENT

The present work was financially supported in part by a Grant-in-Aid for Scientific Research (KAKENHI) on Priority Area (Area No. 477) from the Ministry of Education, Culture, Sports, Science and Technology of Japan to K.I. (22018012) and Y.S. (22018010). This work was also supported by grants from the Japanese Ministry of Education, Culture, Sports, Science, and Technology to K.I., (21770165), Y.S. (22121508), and H.K. (20108014).

■ REFERENCES

(1) Spudich, J. L.; Jung, K.-H. *Handbook of Photosensory Receptors*; Wiley-VCH: Weinheim, 2005.
(2) Chizhov, I.; Schmies, G.; Seidel, R.; Sydor, J. R.; Lüttenberg, B.; Engelhard., M. *Biophys. J.* **1998**, *75*, 999–1009.
(3) Furutani, Y.; Iwamoto, M.; Shimono, K.; Wada, A.; Ito, M.; Kamo, N.; Kandori, H. *Biochemistry* **2004**, *43*, 5204–5212.
(4) Furutani, Y.; Kamada, K.; Sudo, Y.; Shimono, K.; Kamo, N.; Kandori, H. *Biochemistry* **2005**, *44*, 2909–2915.
(5) Gordeliy, V. I.; Labahn, J.; Moukhametzianov, R.; Efremov, R.; Granzin, J.; Schlesinger, R.; Büldt, G.; Savopol, T.; Scheidig, A. J.; Klare, J. P.; Engelhard, M. *Nature* **2002**, *419*, 484–487.
(6) Wegener, A.-A.; Klare, J. P.; Engelhard, M.; Steinhoff, H.-J. *EMBO J.* **2001**, *20*, 5312–5319.
(7) Moukhametzianov, R.; Klare, J. P.; Efremov, R.; Baeken, C.; Göppner, A.; Labahn, J.; Engelhard, M.; Büldt, G.; Gordeliy, V. I. *Nature* **2006**, *440*, 115–119.
(8) Sudo, Y.; Furutani, Y.; Shimono, K.; Kamo, N.; Kandori, H. *Biochemistry* **2003**, *43*, 13748–13754.
(9) Yang, C.-S.; Sineshchekov, O.; Spudich, E. N.; Spudich, J. L. *J. Biol. Chem.* **2004**, *279*, 42970–42976.
(10) Kitajima-Ihara, T.; Furutani, Y.; Suzuki, D.; Ihara, K.; Kandori, H.; Homma, M.; Sudo, Y. *J. Biol. Chem.* **2008**, *283*, 23533–23541.
(11) Yagasaki, J.; Suzuki, D.; Ihara, K.; Inoue, K.; Kikukawa, T.; Sakai, M.; Fujii, M.; Homma, M.; Kandori, H.; Sudo, Y. *Biochemistry* **2010**, *49*, 1183–1190.
(12) Suzuki, D.; Furutani, Y.; Inoue, K.; Kikukawa, T.; Sakai, M.; Fujii, M.; Kandori, H.; Homma, M.; Sudo, Y. *J. Mol. Biol.* **2009**, *392*, 48–62.
(13) Sudo, Y.; Okada, A.; Suzuki, D.; Inoue, K.; Irieda, H.; Sakai, M.; Fujii, M.; Furutani, Y.; Kandori, H.; Homma, M. *Biochemistry* **2009**, *48*, 10136–10145.
(14) Swartz, T. E.; Szundi, I.; Spudich, J. L.; Bogomolni, R. A. *Biochemistry* **2000**, *39*, 15101–15109.
(15) Chizhov, I.; Chernavskii, D. S.; Engelhard, M.; Mueller, K.-H.; Hess, B. *Biophys. J.* **1996**, *71*, 2329–2345.
(16) Lórenz-Fonfría, V. A.; Kandori, H. *J. Am. Chem. Soc.* **2009**, *131*, 5891–5901.
(17) Shibata, M.; Muneda, N.; Sasaki, T.; Shimono, K.; Kamo, N.; Demura, M.; Kandori, H. *Biochemistry* **2005**, *44*, 12279–12286.
(18) Klare, J. P.; Gordeliy, V. I.; Labahn, J.; Büldt, G.; Steinhoff, H.-J.; Engelhard, M. *FEBS Lett.* **2004**, *564*, 219–224.
(19) Garczarek, F.; Gerwert, K. *Nature* **2006**, *439*, 109–112.
(20) Hein, M.; Wegener, A. A.; Engelhard, M.; Siebert, F. *Biophys. J.* **2003**, *84*, 1208–1217.
(21) Hein, M.; Wegener, A. A.; Engelhard, M.; Siebert, F. *Biochemistry* **2004**, *43*, 995–1002.
(22) Lórenz-Fonfría, V. A.; Kandori, H. *Appl. Spectrosc.* **2007**, *61*, 428–443.
(23) Kochendoerfer, G. G.; Kaminaka, S.; Mathies, R. A. *Biochemistry* **1997**, *36*, 13153–13159.
(24) Kim, J. E.; Pan, D.; Mathies, R. A. *Biochemistry* **2003**, *42*, 5169–5175.
(25) Mizuno, M.; Shibata, M.; Yamada, J.; Kandori, H.; Mizutani, Y. *J. Phys.Chem. B* **2009**, *113*, 12121–12128.
(26) Bordignon, E.; Klare, J. P.; Holterhues, J.; Martell, S.; Kransnaberski, A.; Engelhard, M.; Steinhoff, H.-J. *Photochem. Photobiol.* **2007**, *83*, 263–272.
(27) Ostermann, A.; Waschipky, R.; Parak, F. G.; Nienhaus, G. U. *Nature* **2000**, *404*, 205–208.
(28) Schotte, F.; Lim, M.; Jackson, T. A.; Smirnov, A. V.; Soman, J.; Olson, J. S.; Phyillips, G. N., Jr.; Wulff, M.; Anfinrud, P. A. *Science* **2003**, *300*, 1944–1947.
(29) Schmidt, M.; Pahl, R.; Srajer, V.; Anderson, S.; Ren, Z.; Ihee, H.; Rajagopal, S.; Moffat, K. *Proc. Natl. Acad. Sci. U.S.A.* **2004**, *101*, 4799–4804.
(30) Terazima, M.; Hirota, N. *J. Phys. Chem.* **1993**, *97*, 5188–5192.
(31) Sakakura, M.; Morishima, I.; Terazima, M. *J. Phys. Chem. B* **2001**, *105*, 10424–10434.
(32) Takeshita, K.; Imamoto, Y.; Kataoka, M.; Mihara, K.; Tokunaga, F.; Terazima, M. *Biophys. J.* **2002**, *83*, 1567–1577.
(33) Nishida, S.; Nada, T.; Terazima, M. *Biophys. J.* **2004**, *87*, 2663–2675.
(34) Nishioku, Y.; Nakagawa, M.; Tsuda, M.; Terazima, M. *Biophys. J.* **2001**, *80*, 2922–2927.
(35) Inoue, K.; Sasaki, J.; Morisaki, M.; Tokunaga, F.; Terazima, M. *Biophys. J.* **2004**, *87*, 2587–2597.
(36) Inoue, K.; Sasaki, J.; Spudich, J. L.; Terazima, M. *Biophys. J.* **2007**, *92*, 2028–2040.
(37) Inoue, K.; Sasaki, J.; Spudich, J. L.; Terazima, M. *J. Mol. Biol.* **2008**, *376*, 963–970.
(38) Hazra, P.; Inoue, K.; Laan, W.; Hellingwerf, K. J.; Terazima, M. *Biophys. J.* **2006**, *91*, 654–661.
(39) Eitoku, T.; Nakasone, Y.; Matsuoka, D.; Tokutomi, S.; Terazima, M. *J. Am. Chem. Soc.* **2005**, *127*, 13238–13244.
(40) Nakasone, Y.; Eitoku, T.; Matsuoka, D.; Tokutomi, S.; Terazima, M. *J. Mol. Biol.* **2007**, *367*, 432–442.
(41) Tanaka, K.; Nakasone, Y.; Okajima, K.; Ikeuchi, M.; Tokutomi, S.; Terazima, M. *J. Mol. Biol.* **2009**, *386*, 1290–1300.
(42) Losi, A.; Braslavsky, S. E.; Gärtner, W.; Spudich, J. L. *Biophys. J.* **1999**, *76*, 2183–2191.
(43) Hashimoto, S.; Obata, K.; Takeuchi, H.; Needleman, R.; Lanyi, J. K. *Biochemistry* **1997**, *36*, 11583–11590.
(44) Tittor, J.; Oesterhelt, D. *FEBS. Lett.* **1990**, *263*, 269–273.
(45) Inoue, K.; Kubo, M.; Demura, M.; Kamo, N.; Terazima, M. *Biophys. J.* **2009**, *96*, 3724–3734.
(46) Kolbe, M.; Besir, H.; Essen, L.-O.; Oesterhelt, D. *Science* **2000**, *288*, 1390–1396.
(47) Young, M. E.; Carroad, P. A. *Biotechnol. Bioeng.* **1980**, *22*, 947–955.
(48) Møller, J. V.; le Maire, M. *J. Biol. Chem.* **1993**, *268*, 18659–18672.
(49) Salamat-Miller, N.; Chittchang, M.; Mitra, A. K.; Johnston, T. P. *Int. J. Pharm.* **2002**, *244*, 1–8.
(50) Van Holde, K. E.; Johnson, W. C.; Shing Ho, P. *Physical Biochemistry*; Prentice-Hall: Engelwood Cliffs, NJ, USA, 1998.
(51) Chen, X.; Spudich, J. L. *Biochemistry* **2002**, *41*, 3891–3896.
(52) Milligan, D. L.; Koshland, D. E., Jr. *J. Biol. Chem.* **1998**, *263*, 6268–6275.
(53) Zhang, X.-N.; Spudich, J. L. *J. Biol. Chem.* **1998**, *273*, 19722–19728.
(54) Losi, A.; Wegener, A. A.; Engelhard, M.; Gärtner, W.; Braslavsky, S. E. *Biophys. J.* **1999**, *77*, 3277–3286.
(55) Nishioku, Y.; Nakagawa, M.; Tsuda, M.; Terazima, M. *Biophys. J.* **2002**, *83*, 1136–1146.